Antiferromagnetic Bosonic $t-J$ Models and Their Quantum Simulation in Tweezer Arrays

Lukas Homeier,[1,2,3,4,*] Timothy J. Harris,[1,2] Tizian Blatz,[1,2] Sebastian Geier,[5,4] Simon Hollerith,[4] Ulrich Schollwöck,[1,2] Fabian Grusdt,[1,2] and Annabelle Bohrdt[6,2,3,4,†]

[1]*Department of Physics and Arnold Sommerfeld Center for Theoretical Physics (ASC), Ludwig-Maximilians-Universität München, Theresienstr. 37, München D-80333, Germany*

[2]*Munich Center for Quantum Science and Technology (MCQST), Schellingstr. 4, München D-80799, Germany*

[3]*ITAMP, Harvard-Smithsonian Center for Astrophysics, Cambridge, Massachusetts 02138, USA*

[4]*Department of Physics, Harvard University, Cambridge, Massachusetts 02138, USA*

[5]*Physikalisches Institut, Universität Heidelberg, Im Neuenheimer Feld 226, 69120 Heidelberg, Germany*

[6]*Institute of Theoretical Physics, University of Regensburg, Regensburg D-93053, Germany*

(Received 10 May 2023; revised 3 August 2023; accepted 9 May 2024; published 4 June 2024)

The combination of optical tweezer arrays with strong interactions—via dipole exchange of molecules and Van der Waals interactions of Rydberg atoms—has opened the door for the exploration of a wide variety of quantum spin models. A next significant step will be the combination of such settings with mobile dopants. This will enable one to simulate the physics believed to underlie many strongly correlated quantum materials. Here, we propose an experimental scheme to realize bosonic t–J models via encoding the local Hilbert space in a set of three internal atomic or molecular states. By engineering antiferromagnetic (AFM) couplings between spins, competition between charge motion and magnetic order similar to that in high-T_c cuprates can be realized. Since the ground states of the 2D bosonic AFM t–J model we propose to realize have not been studied extensively before, we start by analyzing the case of two dopants—the simplest instance in which their bosonic statistics plays a role—and compare our results to the fermionic case. We perform large-scale density matrix renormalization group calculations on six-legged cylinders, and find a strong tendency for bosonic holes to form stripes. This demonstrates that bosonic, AFM t–J models may contain similar physics as the collective phases in strongly correlated electrons.

DOI: 10.1103/PhysRevLett.132.230401

Introduction.—Trapping, manipulating, and controlling individual qubits in optical tweezer arrays [1–6] has enabled the observation of intriguing many-body physics. Rydberg tweezer platforms stand out with their large Ising or dipolar interaction strengths [7,8], while cold molecules remain coherent for seconds [9] and offer an entire ladder of rotational states [10]. So far, experiments have demonstrated a variety of equilibrium [11,12] and dynamical phenomena [13–16] of quantum magnetism. For example, the toolkit of strong interactions, geometric frustration, and novel readout of nonlocal correlators have revealed topological spin liquid order in Rydberg tweezer arrays [11,17].

One goal of analog quantum simulators is to develop our understanding of the microscopic mechanisms underlying strong correlated quantum matter. Combining spin models with physical tunneling t of particles [18] yields *doped quantum magnets*, where mobile dopants frustrate magnetic order [19] and the statistics of the particles plays a crucial role. Because of its intimate connection to strongly correlated electrons, much effort has been invested in the exploration and quantum gas microscopy of the Fermi-Hubbard model [20,21] with on-site interaction U, using ultracold atoms in optical lattices [22–26]. The underlying superexchange mechanism naturally leads to AFM interactions $J = 4t^2/U$ in fermionic systems, while bosonic models have effective ferromagnetic interactions [19,27].

The behavior of bosonic holes doped into an AFM background raises several interesting questions, but has so far remained elusive due to the ferromagnetic interactions in spin-1/2 Bose-Hubbard models. For example, the microscopic mechanism of hole pairing might not be specific to the Fermi-Hubbard model but instead a universal feature of a broad class of related systems with strong spin-charge correlations, such as the model discussed below.

In this Letter, (i) we study a model combining AFM spin models with mobile (hardcore) bosonic hole dopants in one or two spatial dimensions and (ii) we propose experimental schemes realizing this scenario, suitable for implementation in systems of ultracold polar molecules or Rydberg atoms, where the hole dopants are encoded in the internal degrees of freedom.

In particular, we map a bosonic t–J model [28–34] onto a pure spin model comprised of three Schwinger bosons, which can be implemented hardware-efficiently using the Floquet technique in tweezer systems with dipolar or Van der Waals interactions. Here, the system time evolves under

its natural, e.g., XY interactions followed by a specific sequence of rotations within the three internal states. The effective dynamics of the bosonic excitations is then governed by a t–J Hamiltonian. The tunability enables us to engineer regimes that have not been accessible before, e.g., AFM XXZ interactions, $J > t$, explicit hole-hole (anti) binding potentials or randomized interactions [35].

With the deterministic loading and preparation of product states, time evolution under a tunable Hamiltonian in arbitrary geometry, and ultimately readout by snapshots in the Fock basis, we present a realistic experimental protocol to probe doped bosonic quantum magnets. We highlight the relevance of 2D *bosonic AFM* t–J models by calculating the ground state of a six-legged cylinder doped with two holes using density matrix renormalization group (DMRG). We then compare these results with those obtained from the traditional fermionic t–J model.

Bosonic t–J model as a spin system.—The main ingredient to realize doped spin models, such as the t–J model shown in Fig. 1(a), is a mapping from the original model onto a new model described by Schwinger bosons. The new spin model is then suitable for implementations in established experimental platforms and the desired interactions can be engineered using the Floquet driving technique.

The t–J model describes (hardcore) mobile spin-1/2 particles on a d-dimensional lattice with magnetic interactions; hence, the local Hilbert space is spanned by the hole and *one* particle states $\{|h\rangle, |\downarrow\rangle, |\uparrow\rangle\}$. Here, we investigate bosonic particles $|\sigma\rangle = \hat{a}^\dagger_{j,\sigma}|\mathrm{vac}\rangle$, where we express spins in the Schwinger representation $\hat{\mathbf{S}}_j = \frac{1}{2}\sum_{\sigma,\sigma'} \hat{a}^\dagger_{j,\sigma}\boldsymbol{\tau}_{\sigma,\sigma'}\hat{a}_{j,\sigma'}$ with Pauli matrices $\boldsymbol{\tau} = (\tau^x, \tau^y, \tau^z)$ and $\sigma = \downarrow, \uparrow$. Further, we introduce the (hardcore) bosonic hole operator $|h\rangle = \hat{a}^\dagger_{j,h}|\mathrm{vac}\rangle$.

To obtain the correct Hilbert space, the Schwinger bosons have to fulfill the local constraint

$$\hat{n}^h_j + \hat{n}^\downarrow_j + \hat{n}^\uparrow_j = 1, \tag{1}$$

where $\hat{n}^\sigma_j = \hat{a}^\dagger_{j,\sigma}\hat{a}_{j,\sigma}$ and $\hat{n}^h_j = \hat{a}^\dagger_{j,h}\hat{a}_{j,h}$ are the local spin and hole densities, respectively; see Fig. 1(c).

The bosonic $t-J$ Hamiltonian is given by

$$\begin{aligned}\hat{\mathcal{H}}_{t-J} = &-\sum_{i<j} t_{ij} \sum_\sigma (\hat{a}^\dagger_{i,\sigma}\hat{a}_{i,h}\hat{a}^\dagger_{j,h}\hat{a}_{j,\sigma} + \mathrm{H.c.}) \\ &+ \sum_{i<j}\sum_\alpha J^\alpha_{ij}\hat{S}^\alpha_i\hat{S}^\alpha_j + \sum_{i<j} V_{ij}\hat{n}^h_i\hat{n}^h_j,\end{aligned} \tag{2}$$

with $\alpha = x, y, z$ and the couplings can have arbitrary connectivity and range. The first term $\propto t$ describes tunneling of particles, the second term $\propto J^\alpha$ describes magnetic XXZ interactions with $J^x = J^y = J^\perp$, and the last term $\propto V$ is a hole-hole interaction.

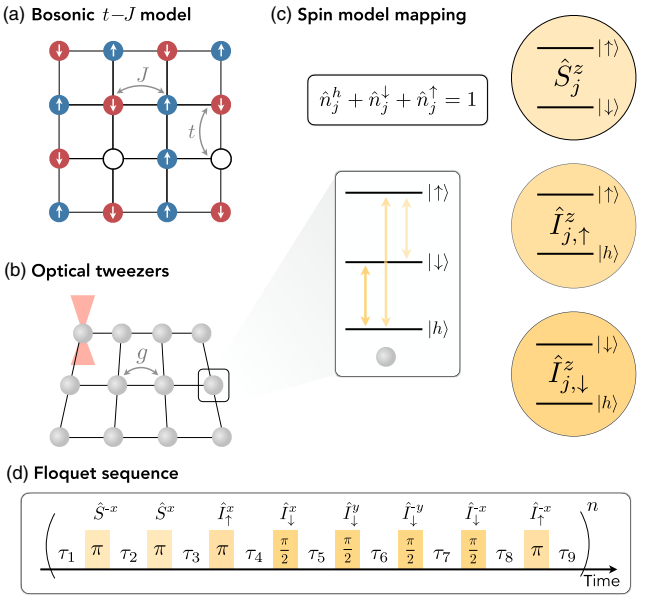

FIG. 1. Schwinger boson mapping. (a) The t–J model describes hopping of spin-1/2 particles on a lattice with tunneling amplitude t together with magnetic interactions J. For AFM interactions, the motion of holes ($|h\rangle$) or particles ($|\downarrow\rangle, |\uparrow\rangle$) frustrates the spin order yielding rich physics for both fermionic and bosonic particles. (b) The latter can be implemented in the internal states of ultracold molecules or Rydberg atoms spatially localized in optical lattices or on an arbitrary graph of tweezer arrays. (c) The local Hilbert space $\{|h\rangle, |\downarrow\rangle, |\uparrow\rangle\}$ can be encoded in the internal rotational states of molecules and we define the three Schwinger spins $\hat{\mathbf{S}}$, $\hat{\mathbf{I}}_\uparrow$, and $\hat{\mathbf{I}}_\downarrow$, which allows us to exactly represent the t–J Hamiltonian as a spin model. (d) In the isolated three-level subspace of rotational states $|N\rangle$ with $N = 0, 1, 2$, the molecular Hamiltonian we consider has XY interactions between $N = 0, 1$. By performing periodic rotations on the $\hat{\mathbf{S}}$- and $\hat{\mathbf{I}}_\sigma$-Bloch spheres, the effective Floquet Hamiltonian in spin representation can be engineered. The duration τ_n of individual Floquet evolution steps determines the effective coupling strengths of the target Hamiltonian (4) (here with $V = 0$).

The model (2) gains its importance because it captures the low-energy effective theory of the repulsive Fermi- or Bose-Hubbard models in the strong coupling regime $U \gg t$ [19]. However, the perturbative derivation exactly determines the couplings, which for nearest-neighbor (NN) hopping are given by $J^\alpha = \pm 4t^2/U$ and $V = -J(\pm 2 - 1)/4$ for the fermionic (+) or bosonic (−) models, respectively.

Our proposed scheme for realizing the model (2) in experiment enables broad tunability [36,37] of the Hamiltonian parameters. In particular, the ability to tune the ratio between the hole-hole interaction V and magnetic interactions J in our model facilitates exploration of potentially interesting pairing regimes, which we study numerically in the second part of this Letter.

First, we perform an exact mapping of Hamiltonian (2) onto a new XXZ spin model composed of the three spin-1/2 Schwinger spins $\hat{\mathbf{S}}_j$, $\hat{\mathbf{I}}_{j,\downarrow}$, and $\hat{\mathbf{I}}_{j,\uparrow}$ with

$$\hat{S}^z_j = \frac{1}{2}\left(\hat{n}^\uparrow_j - \hat{n}^\downarrow_j\right) \quad \hat{S}^+_j = \hat{a}^\dagger_{j,\uparrow}\hat{a}_{j,\downarrow}$$
$$\hat{I}^z_{j,\sigma} = \frac{1}{2}(\hat{n}^\sigma_j - \hat{n}^h_j) \quad \hat{I}^+_{j,\sigma} = \hat{a}^\dagger_{j,\sigma}\hat{a}_{j,h}, \tag{3}$$

from which we obtain (up to a constant energy shift)

$$\hat{\mathcal{H}}_{t\text{–}J} = -\sum_{i<j}\sum_{\alpha,\sigma} t^\alpha_{ij}\hat{I}^\alpha_{i,\sigma}\hat{I}^\alpha_{j,\sigma} + \sum_{i<j}\sum_{\alpha} g^\alpha_{ij}\hat{S}^\alpha_i\hat{S}^\alpha_j. \tag{4}$$

We neglect a chemical potential term for the holes since we assume the total number of particles is conserved. The form of Eq. (4) is very useful for our proposed implementation below, but we emphasize that the Schwinger spins are not mutually independent, i.e., $[\hat{S}^z_j, \hat{I}^\pm_{j,\sigma}] \neq 0$.

The hole-hole interaction renormalizes the XXZ models and we find the following couplings related to Eq. (2) and (4):

$$t^x_{ij} = t^y_{ij} = \frac{1}{2}t_{ij} \quad t^z_{ij} = -\frac{8}{9}V_{ij}$$
$$g^x_{ij} = g^y_{ij} = J^\perp_{ij} \quad g^z_{ij} = J^z_{ij} - \frac{4}{9}V_{ij}. \tag{5}$$

So far, we have performed exact transformations and rewritten the t–J model in terms of Schwinger bosons. The Schwinger spins have to fulfill the number constraint (1), which induces highly nontrivial spin-charge correlations and thus is beyond a simple spin-1/2 chain. Likewise, the construction can be formulated in terms of mutually hardcore bosonic statistics, i.e., $\hat{a}^\dagger_{j,\Sigma}\hat{a}^\dagger_{j,\Sigma'} = 0$ for $\Sigma = \downarrow, \uparrow, h$.

The constraint can be elegantly implemented in a spin-1 manifold in, e.g., ultracold molecule or Rydberg tweezer arrays. To this end, we propose two schemes, which either utilize dipolar spin exchange interactions to engineer the desired dynamics by Floquet driving, or directly enable the realization of Hamiltonian (4) in three isolated Rydberg states.

Experimental proposal: Ultracold molecules.—Ultracold polar molecules have recently demonstrated the realization of an anisotropic XXZ model in a qubit subspace of rotational states [16], which can be achieved by Floquet engineering. There, the system consecutively time evolves under the resonant dipole-dipole interactions followed by fast qubit rotations, i.e., driving microwave transitions between rotational states.

Here, we extend the scheme by using three states in the rotational manifold $|N\rangle$ with $N = 0, 1, 2$ and we identify the molecular states $\{|0\rangle, |1\rangle, |2\rangle\}$ with the local Hilbert space $\{|h\rangle, |\downarrow\rangle, |\uparrow\rangle\}$ of the t–J model. The molecular Hamiltonian expressed in terms of the Schwinger spins (3) is given by

$$\hat{\mathcal{H}}_{\text{mol}} = \sum_{i<j}\chi_{ij}(\hat{I}^+_{i,\downarrow}\hat{I}^-_{j,\downarrow} + \text{H.c.}), \tag{6}$$

with $\chi_{ij} = \chi(1 - 3\cos^2\theta_{ij})/|\mathbf{r}_{ij}|^3$. Here, $\mathbf{r}_{ij}$ is the vector connecting lattice sites i and j, and θ_{ij} is the angle between the quantization axis and $\mathbf{r}_{ij}$. In the following, we choose $\theta_{ij} = \pi/2$ and set the NN distance to $r_{ij} \equiv 1$. The XY coupling strength χ, is determined by the resonant dipole moments of the molecule [10,38], and here we only consider interactions between $N = 0$, 1 [39], while the state $N = 2$ is noninteracting. This can be achieved by using the selection rules $\Delta m_N = 0, \pm 1$ of the dipole interactions, e.g., we propose to use $|N = 0, m_N = 0\rangle$, $|N = 1, m_N = 0\rangle$, and $|N = 2, m_N = -2\rangle$.

Next, we describe a scheme to realize a t–J model with tunable XXZ magnetic interactions. To this end, we consider the molecular Hamiltonian (6) with flip-flop interactions χ_{ij}. By comparing this model to the t–J Hamiltonian (4), we find that the microscopic model corresponds to a t–J model with tunneling of $|\downarrow\rangle$ particles only. Hence, we propose to perform consecutive, fast rotations between all pairs of states, i.e., on the $\hat{\mathbf{I}}_\sigma$- and $\hat{\mathbf{S}}$-Bloch spheres, to obtain a time-averaged Hamiltonian with equal strength $|\uparrow\rangle$- and $|\downarrow\rangle$-particle tunneling. The sequence of Floquet rotations is shown in Fig. 1(d): tuning the times τ_n of Floquet steps allows for the implementation of models with tunable ratios $-t/J^z > 0$ and $J^\perp/J^z > 0$ ($J_z > 0$) and $V = 0$. This result holds in first-order Floquet theory and is derived in the Supplemental Material [40]; a comparison between the target t–J model and Floquet time evolution using exact diagonalization shows excellent agreement and demonstrates the robustness of our proposed scheme.

We emphasize that the long-range interactions directly transfer to the effective model and hence a t–J model with r^{-3} tails is realized in cold molecules. Enriching the Floquet protocol by spatial rearrangements [41], pure NN interactions or even models with arbitrary connectivity can be implemented in principle. Depending on the stability of dc electric fields, the fidelity of microwave transitions and coherence times across multiple rotational levels [42,43], effective Floquet Hamiltonians [44] of differing complexity can be realized; in particular in the Supplemental Material we present a Floquet sequence that gives rise to t–J–V models with $0 < V/J^z < 9/4$ and $J^\perp/J^z > 1/2$.

Experimental proposal: Rydberg tweezer arrays.—Rydberg atoms in optical lattices [45] and tweezer arrays have become an established platform in the quantum simulation of magnetism [7,8,11,12,14,15]. In particular, tunable spin-1/2 XXZ models have previously been realized via Rydberg dressing [46], Floquet engineering [47,48], and precise selection of Rydberg states [49].

The proposed model (4) requires control over interactions within a three-level system. We propose a direct implementation within three Rydberg states by identifying

$$|nS\rangle = |\downarrow\rangle \quad |n'P\rangle = |h\rangle \quad |n''S\rangle = |\uparrow\rangle. \tag{7}$$

The resonant dipolar exchange between states of different parity implements long-ranged tunnelings, e.g., the exchange interaction between the pair of atoms $|nS_i, n'P_j\rangle \leftrightarrow |n'P_i, nS_j\rangle$ at site i and j corresponds to tunneling of $\downarrow$ particles with amplitude $t_{ij}^{\downarrow} \propto r_{ij}^{-3}$. Models with either approximate SU(2) invariant tunnelings or spin-dependent tunnelings can be implemented.

Further, the spin interactions can be induced by choosing suitable pair states $|nS, n''S\rangle$, such that the resulting Van der Waals interactions $\propto r^{-6}$ give rise to flip-flop $J_\perp$ and Ising terms J_z [50], as demonstrated in Ref. [49]. Notably, the different scaling behaviors of the tunneling and spin interactions allow us to tune the ratio of t/J over a wide range.

In the (exact) mapping from the Rydberg Hamiltonian onto the spin model, additional terms appear from the anisotropy in the diagonal Van der Waals interaction between pair states. These terms give rise to a t–J–V–W model [see Eq. (2)] with spin-hole interactions $\propto W_{ij}\hat{n}_i^h\hat{S}_j^z$. Using the states from Ref. [49], we find the latter to be negligible.

Spin-charge order in the bosonic t–J model.— Understanding the nature of mobile dopants in strongly correlated phases of matter has a long history, motivated by high-T_c superconductors and more recently by layered 2D materials [51]. The fate of the AFM Mott insulator under doping is still debated; however, experiments in cuprates have revealed that even a few percent of fermionic dopants can lead to a robust d-wave superconducting ground state [20,52]. Hence, strong pairing of charge carriers—the hole dopants—mediated by magnetic interactions [53] likely plays a key role.

Here, we perform a first numerical study of hole dopants in the ground state of the 2D bosonic AFM t–J model, comparing our results to an equivalent calculation using the standard fermionic t–J model. Let us emphasize that previous studies of the bosonic t–J model have considered either lower dimensions, high temperature expansions or *partial* AFM couplings ($J^z > 0, J^\perp \leq 0$) [28–34]. In contrast, our model takes a further step toward strongly correlated materials by studying fully antiferromagnetic interactions in the spin sector ($J^z, J^\perp > 0$) with the cost of introducing a sign problem at low temperatures; there our model is intractable for large-scale quantum Monte Carlo simulations.

To this end, the ground state with two holes in the zero-magnetization sector, $\hat{S}_z = 0$, of the SU(2)-invariant version of Eq. (2), $J^\alpha \equiv J$, was obtained from DMRG calculations on a long cylinder [54–57]; the interactions are restricted to NN and have strength $t/J = 2$ and $V/J = -1/4$ (see Supplemental Material). To analyze the structure of the obtained pair wave functions, we extract (i) the reduced hole-hole correlation $\langle \hat{n}_i^h \hat{n}_j^h \rangle / \langle \hat{n}_i^h \rangle \langle \hat{n}_j^h \rangle$ and (ii) the spin-spin correlation $\langle \hat{S}_i^z \hat{S}_j^z \rangle$ functions shown in Fig. 2.

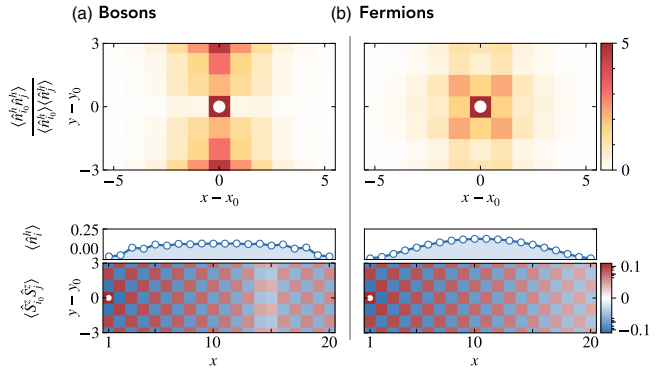

FIG. 2. Bosonic vs fermionic two-hole states. We show ground-state correlation functions for a t–J model with two (a) bosonic and (b) fermionic holes obtained from DMRG calculations on 20×6 cylinders. We find distinctly different behavior for bosons and fermions by evaluating the hole-hole (top) and spin-spin correlation functions (bottom). (a) The hole-hole correlator, centered around its reference site, $\boldsymbol{i}_0 = (x_0 = 10, y_0 = 3)$, shows a charge-density wave pattern around the short direction of the cylinder. Additionally, we find a domain wall in the spin-spin correlation function with reference site $\boldsymbol{i}_0 = (x_0 = 1, y_0 = 3)$, on the boundary (white dot); hence the bosons form a stripe. (b) The fermions are tightly bound into an isotropic pair embedded in a homogeneous AFM background. For both statistics, we plot the hole density averaged around the short direction of the cylinder, which also serves as a marker for convergence of our results (see Supplemental Material).

The well-known case of fermionic holes [52,58,59] indicates the formation of a tightly bound pair state, which can be seen from the C4-symmetric hole-hole correlations [Fig. 2(b), top] and the absence of a spin domain wall across the hole-rich region [Fig. 2(b), bottom]. While the intuitive picture for bosons suggests the holes to condense and similarly bunch together, we find a surprising situation: the bosons have a tendency toward stripe formation. At finite density of holes, such stripes form in, e.g., cuprate materials, describing periodic charge modulations bound to π-phase shifts of the spin-spin correlations (domain walls) across the hole-rich regions.

In our small system simulation, the two bosonic holes show strong tendency to pair along the short, periodic direction of the cylinder, as evident from the hole-hole correlations [Fig. 2(a), top]. In contrast to the fermionic case, we observe a spin domain wall across the hole-rich region [Fig. 2(a), bottom], a hallmark of stripe formation. Additionally, the charge correlations show short-range repulsion along the short direction, distinctly different from the structure of the C4-invariant pair of the fermionic holes but resembling the situation in a stripe. Both scenarios, tightly bound pairs and stripe correlations, are marking phases observed in strongly correlated electrons [52,60].

This minimal instance—comparing two-hole fermionic and bosonic states—already shows rich phenomenology

and demonstrates an intriguing first experimental application of our proposal. Future experimental and numerical studies of the bosonic AFM t–J model can be expected to provide a fresh perspective from which to advance our current understanding of the physics of doped Mott insulators.

Experimental probes.—In the following, we discuss observables that can be obtained from snapshots in our proposed experimental scheme. From low to high doping, we suggest a number of useful probes: single-hole angle-resolved photoemission spectroscopy, binding energies, $g^{(2)}$ correlation functions, and transport.

A single-hole dopant in an AFM background forms a quasiparticle, the magnetic polaron, with rich internal structure [61]. Previous experiments focused on measurements of hole-spin-spin correlation functions [25] or dynamical probes [62]. However, a plethora of ro-vibrational excitation modes are predicted from numerical calculations [63], which could be revealed by single-hole angle-resolved photoemission spectroscopy [64]. In our proposed model, a momentum-insensitive yet spin-selective measurement can be easily performed by driving microwave transitions between the $|\downarrow\rangle$ ($|\uparrow\rangle$) and $|h\rangle$ states, in order to evaluate the transition probabilities. We note that in the $t-J^z$ model ($J^\perp = 0$) the energy is approximately momentum-independent; in our proposed scheme this can be implemented as a limit of the XXZ model with strong Ising terms. Moreover, the characteristic excitation spectrum of the single hole is a staircase of string-excited states [61,65–67] with energies scaling as $t^{1/3}(J^z)^{2/3}$, which could be directly probed by momentum-independent measurements.

In contrast to optical lattice experiments, platforms utilizing tweezer arrays allow for direct access to energies $\langle\hat{\mathcal{H}}\rangle$ by taking snapshots in the different bases of $\hat{S}^\alpha$ and $\hat{I}^\alpha_\sigma$ and evaluating the terms individually in Hamiltonian (4). The experimental protocol first requires an adiabatic state preparation protocol, e.g., by preparing a deterministic, low-energy Néel state followed by tuning suitable parameters. Repeating the experiment for zero, one, and two holes then allows one to measure, e.g., their binding energy directly.

On the other hand, indirect signatures of pairing or stripe formation can be obtained from $g^{(2)}$ correlation functions. Moreover, the tunability of our model may give a new perspective on the nature of the ground state. In particular, tuning the magnetic or hole-hole interaction V can (un) favor pairing, which manifests in the hole-hole distance. Moreover, at finite doping we speculate that the phase diagram—similar to its fermionic counterpart—hosts instabilities toward incommensurate charge and spin ordered phases of matter. Hence, the formation (or absence) of stripes at finite doping with its correlation between density and spin domain walls can be investigated from state-dependent snapshots.

Lastly, we suggest to probe spin and charge transport by time-evolving an initial product state, e.g., a charge-density wave [68]. The control of atoms on the single-particle level in tweezer arrays [8] naturally suggests to apply quench protocols to an initial product state. Studying transport properties in 2D t–J models with long-range interactions and at finite doping could give important insights into exotic phases of matter with potential connections to strange metallicity.

Discussion and outlook.—We have studied a class of models where AFM interactions are combined with bosonic hole dopants in 2D. Our proposed model is of particular interest due to the prospect of near-term realizations in analog quantum simulation experiments. While we have predominantly discussed schemes for analog quantum simulation, we also envisage future applications in hybrid digital-analog platforms [69], where fast physical tunneling of bosonic or fermionic (Rydberg) atoms can be realized. Further, extensions in other three-manifolds of circular Rydberg states may be possible [70].

We demonstrated the relevance for strongly correlated materials and potential connections to high-T_c superconductivity using state-of-the-art numerical techniques; this motivates future theoretical, numerical, and experimental studies of bosonic AFM t–J models. Additionally, the precise tunability of our proposed model opens exciting new avenues to explore pairing mechanisms and collective phases of doped Mott insulators [71]. For example, via tuning the hole-hole interaction to realize a hole binding-unbinding transition. Lastly, the experimental building block could enable the realization of more elaborate strongly correlated systems, e.g., non-Abelian lattice gauge theories [72].

Note added.—During the publication process, we became aware of a tunable, fermionic t–J model implemented in cold molecules using physical tunneling of molecules in a lattice [73].

We are very grateful to K.-K. Ni, A. Park, G. Patenotte, and L. Picard for fruitful discussions and insights regarding the cold molecule scheme, and we wish to thank N.-C. Chiu for valuable feedback on Rydberg atom implementations. We thank D. Wei and J. Zeiher for insightful discussions. L. H. acknowledges support from the Studienstiftung des deutschen Volkes. T. J. H. acknowledges funding by the Munich Quantum Valley (MQV) doctoral fellowship program, which is supported by the Bavarian state government with funds from the Hightech Agenda Bayern Plus. S. H. acknowledges funding through the Harvard Quantum Initiative Postdoctoral Fellowship in Quantum Science and Engineering. This research was funded by the Deutsche Forschungsgemeinschaft (DFG, German Research Foundation) under Germany's Excellence Strategy—EXC-2111–390814868, by the European Research Council (ERC) under the European Union's

Horizon 2020 research and innovation programme (Grant agreement No. 948141), by the NSF through a grant for the Institute for Theoretical Atomic, Molecular, and Optical Physics at Harvard University and the Smithsonian Astrophysical Observatory.

*Corresponding author: lukas.homeier@physik.uni-muenchen.de
†Corresponding author: annabelle.bohrdt@physik.uni-regensburg.de

[1] M. Endres, H. Bernien, A. Keesling, H. Levine, E. R. Anschuetz, A. Krajenbrink, C. Senko, V. Vuletic, M. Greiner, and M. D. Lukin, Science **354**, 1024 (2016).
[2] L. Anderegg, L. W. Cheuk, Y. Bao, S. Burchesky, W. Ketterle, K.-K. Ni, and J. M. Doyle, Science **365**, 1156 (2019).
[3] A. M. Kaufman and K.-K. Ni, Nat. Phys. **17**, 1324 (2021).
[4] A. Browaeys and T. Lahaye, Nat. Phys. **16**, 132 (2020).
[5] C. M. Holland, Y. Lu, and L. W. Cheuk, Science **382**, 1143 (2023).
[6] J. T. Zhang, L. R. B. Picard, W. B. Cairncross, K. Wang, Y. Yu, F. Fang, and K.-K. Ni, Quantum Sci. Technol. **7**, 035006 (2022).
[7] S. de Léséleuc, V. Lienhard, P. Scholl, D. Barredo, S. Weber, N. Lang, H. P. Büchler, T. Lahaye, and A. Browaeys, Science **365**, 775 (2019).
[8] C. Chen, G. Bornet, M. Bintz, G. Emperauger, L. Leclerc, V. S. Liu, P. Scholl, D. Barredo, J. Hauschild, S. Chatterjee, M. Schuler, A. M. Läuchli, M. P. Zaletel, T. Lahaye, N. Y. Yao, and A. Browaeys, Nature (London) **616**, 691 (2023).
[9] P. D. Gregory, J. A. Blackmore, S. L. Bromley, J. M. Hutson, and S. L. Cornish, Nat. Phys. **17**, 1149 (2021).
[10] B. Sundar, B. Gadway, and K. R. A. Hazzard, Sci. Rep. **8**, 3422 (2018).
[11] G. Semeghini, H. Levine, A. Keesling, S. Ebadi, T. T. Wang, D. Bluvstein, R. Verresen, H. Pichler, M. Kalinowski, R. Samajdar, A. Omran, S. Sachdev, A. Vishwanath, M. Greiner, V. Vuletić, and M. D. Lukin, Science **374**, 1242 (2021).
[12] S. Ebadi, T. T. Wang, H. Levine, A. Keesling, G. Semeghini, A. Omran, D. Bluvstein, R. Samajdar, H. Pichler, W. W. Ho, S. Choi, S. Sachdev, M. Greiner, V. Vuletić, and M. D. Lukin, Nature (London) **595**, 227 (2021).
[13] B. Yan, S. A. Moses, B. Gadway, J. P. Covey, K. R. A. Hazzard, A. M. Rey, D. S. Jin, and J. Ye, Nature (London) **501**, 521 (2013).
[14] H. Bernien, S. Schwartz, A. Keesling, H. Levine, A. Omran, H. Pichler, S. Choi, A. S. Zibrov, M. Endres, M. Greiner, V. Vuletić, and M. D. Lukin, Nature (London) **551**, 579 (2017).
[15] A. Keesling, A. Omran, H. Levine, H. Bernien, H. Pichler, S. Choi, R. Samajdar, S. Schwartz, P. Silvi, S. Sachdev, P. Zoller, M. Endres, M. Greiner, V. Vuletić, and M. D. Lukin, Nature (London) **568**, 207 (2019).
[16] L. Christakis, J. S. Rosenberg, R. Raj, S. Chi, A. Morningstar, D. A. Huse, Z. Z. Yan, and W. S. Bakr, Nature (London) **614**, 64 (2023).
[17] R. Verresen, M. D. Lukin, and A. Vishwanath, Phys. Rev. X **11**, 031005 (2021).
[18] A. M. Kaufman, B. J. Lester, C. M. Reynolds, M. L. Wall, M. Foss-Feig, K. R. A. Hazzard, A. M. Rey, and C. A. Regal, Science **345**, 306 (2014).
[19] A. Auerbach, *Interacting Electrons and Quantum Magnetism* (Springer, New York, 1994).
[20] B. Keimer, S. A. Kivelson, M. R. Norman, S. Uchida, and J. Zaanen, Nature (London) **518**, 179 (2015).
[21] A. Bohrdt, L. Homeier, C. Reinmoser, E. Demler, and F. Grusdt, Ann. Phys. (Amsterdam) **435**, 168651 (2021).
[22] L. W. Cheuk, M. A. Nichols, K. R. Lawrence, M. Okan, H. Zhang, E. Khatami, N. Trivedi, T. Paiva, M. Rigol, and M. W. Zwierlein, Science **353**, 1260 (2016).
[23] D. Mitra, P. T. Brown, E. Guardado-Sanchez, S. S. Kondov, T. Devakul, D. A. Huse, P. Schauß, and W. S. Bakr, Nat. Phys. **14**, 173 (2017).
[24] A. Mazurenko, C. S. Chiu, G. Ji, M. F. Parsons, M. Kanász-Nagy, R. Schmidt, F. Grusdt, E. Demler, D. Greif, and M. Greiner, Nature (London) **545**, 462 (2017).
[25] J. Koepsell, J. Vijayan, P. Sompet, F. Grusdt, T. A. Hilker, E. Demler, G. Salomon, I. Bloch, and C. Gross, Nature (London) **572**, 358 (2019).
[26] M. Xu, L. H. Kendrick, A. Kale, Y. Gang, G. Ji, R. T. Scalettar, M. Lebrat, and M. Greiner, Nature (London) **620**, 971 (2023).
[27] L.-M. Duan, E. Demler, and M. D. Lukin, Phys. Rev. Lett. **91**, 090402 (2003).
[28] J. Šmakov, C. D. Batista, and G. Ortiz, Phys. Rev. Lett. **93**, 067201 (2004).
[29] M. Boninsegni and N. V. Prokof'ev, Phys. Rev. B **77**, 092502 (2008).
[30] K. Aoki, K. Sakakibara, I. Ichinose, and T. Matsui, Phys. Rev. B **80**, 144510 (2009).
[31] Y. Nakano, T. Ishima, N. Kobayashi, K. Sakakibara, I. Ichinose, and T. Matsui, Phys. Rev. B **83**, 235116 (2011).
[32] Y. Nakano, T. Ishima, N. Kobayashi, T. Yamamoto, I. Ichinose, and T. Matsui, Phys. Rev. A **85**, 023617 (2012).
[33] H. Sun, B. Yang, H.-Y. Wang, Z.-Y. Zhou, G.-X. Su, H.-N. Dai, Z.-S. Yuan, and J.-W. Pan, Nat. Phys. **17**, 990 (2021).
[34] P. N. Jepsen, W. W. Ho, J. Amato-Grill, I. Dimitrova, E. Demler, and W. Ketterle, Phys. Rev. X **11**, 041054 (2021).
[35] M. Christos, D. G. Joshi, S. Sachdev, and M. Tikhanovskaya, Proc. Natl. Acad. Sci. U.S.A. **119** (2022).
[36] A. V. Gorshkov, S. R. Manmana, G. Chen, J. Ye, E. Demler, M. D. Lukin, and A. M. Rey, Phys. Rev. Lett. **107**, 115301 (2011).
[37] J. R. Coulthard, S. R. Clark, S. Al-Assam, A. Cavalleri, and D. Jaksch, Phys. Rev. B **96**, 085104 (2017).
[38] M. L. Wall, K. R. A. Hazzard, and A. M. Rey, in *From Atomic to Mesoscale* (World Scientific, Singapore, 2015), pp. 3–37.
[39] A. J. Park, L. R. B. Picard, G. E. Patenotte, J. T. Zhang, T. Rosenband, and K.-K. Ni, Phys. Rev. Lett. **131**, 183401 (2023).
[40] See Supplemental Material at http://link.aps.org/supplemental/10.1103/PhysRevLett.132.230401 for additional information about the implementation in polar molecules. We describe details of the Floquet sequence and provide numerical simulations. Further, we give additional details about and show the convergence of the density-matrix renormalization group studies.

[41] D. Bluvstein, H. Levine, G. Semeghini, T. T. Wang, S. Ebadi, M. Kalinowski, A. Keesling, N. Maskara, H. Pichler, M. Greiner, V. Vuletić, and M. D. Lukin, Nature (London) **604**, 451 (2022).
[42] K.-K. Ni, T. Rosenband, and D. D. Grimes, Chem. Sci. **9**, 6830 (2018).
[43] T. Rosenband, D. D. Grimes, and K.-K. Ni, Opt. Express **26**, 19821 (2018).
[44] B.-Y. Sun, N. Goldman, M. Aidelsburger, and M. Bukov, PRX Quantum **4**, 020329 (2023).
[45] J. Zeiher, R. van Bijnen, P. Schauß, S. Hild, J. yoon Choi, T. Pohl, I. Bloch, and C. Gross, Nat. Phys. **12**, 1095 (2016).
[46] L.-M. Steinert, P. Osterholz, R. Eberhard, L. Festa, N. Lorenz, Z. Chen, A. Trautmann, and C. Gross, Phys. Rev. Lett. **130**, 243001 (2023).
[47] S. Geier, N. Thaicharoen, C. Hainaut, T. Franz, A. Salzinger, A. Tebben, D. Grimshandl, G. Zürn, and M. Weidemüller, Science **374**, 1149 (2021).
[48] P. Scholl, H. J. Williams, G. Bornet, F. Wallner, D. Barredo, L. Henriet, A. Signoles, C. Hainaut, T. Franz, S. Geier, A. Tebben, A. Salzinger, G. Zürn, T. Lahaye, M. Weidemüller, and A. Browaeys, PRX Quantum **3**, 020303 (2022).
[49] T. Franz, S. Geier, C. Hainaut, N. Thaicharoen, A. Braemer, M. Gärttner, G. Zürn, and M. Weidemüller, arXiv:2209.08080.
[50] S. Whitlock, A. W. Glaetzle, and P. Hannaford, J. Phys. B **50**, 074001 (2017).
[51] Y. Cao, V. Fatemi, S. Fang, K. Watanabe, T. Taniguchi, E. Kaxiras, and P. Jarillo-Herrero, Nature (London) **556**, 43 (2018).
[52] H. Xu, C.-M. Chung, M. Qin, U. Schollwöck, S. R. White, and S. Zhang, Science **384**, eadh7691 (2024).
[53] S. M. O'Mahony, W. Ren, W. Chen, Y. X. Chong, X. Liu, H. Eisaki, S. Uchida, M. H. Hamidian, and J. C. S. Davis, Proc. Natl. Acad. Sci. U.S.A. **119** (2022).
[54] S. R. White, Phys. Rev. Lett. **69**, 2863 (1992).
[55] U. Schollwöck, Ann. Phys. (Amsterdam) **326**, 96 (2011).
[56] C. Hubig, Symmetry-protected tensor networks, Ph. D. thesis, Ludwig-Maximilians Universität, 2017.
[57] C. Hubig, F. Lachenmaier, N.-O. Linden, T. Reinhard, L. Stenzel, A. Swoboda, and M. Grundner, The SYTEN toolkit, https://syten.eu.
[58] M. Qin, C.-M. Chung, H. Shi, E. Vitali, C. Hubig, U. Schollwöck, S. R. White, and S. Z. and, Phys. Rev. X **10**, 031016 (2020).
[59] X. Lu, F. Chen, W. Zhu, D. N. Sheng, and S.-S. Gong, Phys. Rev. Lett. **132**, 066002 (2024).
[60] A. Wietek, Y.-Y. He, S. R. White, A. Georges, and E. M. Stoudenmire, Phys. Rev. X **11**, 031007 (2021).
[61] F. Grusdt, M. Kánasz-Nagy, A. Bohrdt, C. S. Chiu, G. Ji, M. Greiner, D. Greif, and E. Demler, Phys. Rev. X **8**, 011046 (2018).
[62] G. Ji, M. Xu, L. H. Kendrick, C. S. Chiu, J. C. Brüggenjürgen, D. Greif, A. Bohrdt, F. Grusdt, E. Demler, M. Lebrat, and M. Greiner, Phys. Rev. X **11**, 021022 (2021).
[63] A. Bohrdt, E. Demler, and F. Grusdt, Phys. Rev. Lett. **127**, 197004 (2021).
[64] P. T. Brown, E. Guardado-Sanchez, B. M. Spar, E. W. Huang, T. P. Devereaux, and W. S. Bakr, Nat. Phys. **16**, 26 (2019).
[65] S. A. Trugman, Phys. Rev. B **37**, 1597 (1988).
[66] C. L. Kane, P. A. Lee, and N. Read, Phys. Rev. B **39**, 6880 (1989).
[67] P. Wrzosek and K. Wohlfeld, Phys. Rev. B **103**, 035113 (2021).
[68] P. T. Brown, D. Mitra, E. Guardado-Sanchez, R. Nourafkan, A. Reymbaut, C.-D. Hébert, S. Bergeron, A.-M. S. Tremblay, J. Kokalj, D. A. Huse, P. Schauß, and W. S. Bakr, Science **363**, 379 (2019).
[69] D. González-Cuadra, D. Bluvstein, M. Kalinowski, R. Kaubruegger, N. Maskara, P. Naldesi, T. V. Zache, A. M. Kaufman, M. D. Lukin, H. Pichler, B. Vermersch, J. Ye, and P. Zoller, Proc. Natl. Acad. Sci. U.S.A. **120** (2023).
[70] A. Kruckenhauser, R. van Bijnen, T. V. Zache, M. D. Liberto, and P. Zoller, Quantum Sci. Technol. **8**, 015020 (2022).
[71] P. A. Lee, N. Nagaosa, and X.-G. Wen, Rev. Mod. Phys. **78**, 17 (2006).
[72] J. C. Halimeh*, L. Homeier*, A. Bohrdt, and F. Grusdt, arXiv:2305.06373.
[73] A. N. Carroll, H. Hirzler, C. Miller, D. Wellnitz, S. R. Muleady, J. Lin, K. P. Zamarski, R. R. W. Wang, J. L. Bohn, A. M. Rey, and J. Ye, arXiv:2404.18916.